COMPUTATIONAL AND EXPERIMENTAL EVALUATION OF AIRFLOW BEHAVIOR AND THERMAL COMFORT IN A CASSETTE AIR-CONDITIONED CLASSROOM

Ba-Loc Le[1], Duc-Khanh Nguyen[2], Le-Quang Dang[3]*

[1]National Central University (NCU), Taiwan
[2]Ho Chi Minh City University of Technology, Vietnam National University Ho Chi Minh City (VNU-HCM), Vietnam
[3]Foreign Trade University, Ho Chi Minh City Campus II, Vietnam

*Corresponding author: danglequang.cs2@ftu.edu.vn

(Received: December 26, 2025; Revised: April 19, 2026; Accepted: May 29, 2026)

DOI: 10.31130/ud-jst.2026.24(6A).733

Abstract - This study evaluates thermal comfort and airflow characteristics of an HVAC system in a university classroom to improve indoor thermal environmental quality. A cassette air-conditioner layout was analyzed using Computational Fluid Dynamics (CFD) simulations conducted with Ansys Fluent. The simulations investigated supply air outlet angles of 15°, 30°, and 45° with inlet velocities ranging from 1.22 m/s to 1.92 m/s. The results indicate that airflow velocity and supply air temperature significantly influence airflow distribution and thermal comfort. Within the investigations, an inlet air velocity of 1.56 m/s with a 60° discharge angle provided a good balance between cooling performance, thermal uniformity, and occupant comfort. The low supply air temperature cases were employed to investigate trends in airflow organization and temperature distribution, rather than to recommend long-term operating conditions for the HVAC systems.

Key words - Thermal comfort; Airflow distribution; HVAC system; Cassette air conditioner; Computational Fluid Dynamics (CFD)

1. Introduction

Thermal comfort is an important factor that directly affects human health, cognitive ability, and productivity; therefore, it has become a central research topic in building design, indoor environmental engineering, and occupational health. Thermal comfort reflects the subjective perception of occupants toward the thermal environment and is influenced by temperature, humidity, air movement, clothing, and metabolic rate. Inappropriate thermal conditions can reduce concentration, learning performance, and occupant satisfaction [1]. Therefore, the assessment of thermal comfort requires not only consideration of the physical characteristics of the indoor environment but also the physiological responses and behavioral factors of occupants.

Standards such as ISO 7730 and ASHRAE Standard 55 provide a systematic assessment framework for thermal comfort and emphasize the balance between energy efficiency and occupant comfort [1], [2]. Thermal comfort is defined as "the condition of mind that expresses satisfaction with the thermal environment." Thermal comfort is affected by six main factors, including four environmental factors, namely air temperature, mean radiant temperature, air velocity, and humidity, and two personal factors, namely metabolic rate and clothing insulation.

This issue has become increasingly urgent in educational facilities, particularly in hot and humid climates, where cooling demand is high and HVAC systems must operate under severe conditions. Many studies have applied computational fluid dynamics (CFD) to analyze temperature distribution, airflow patterns, and HVAC system performance in classrooms. The results indicate that the air supply method, location, and diffuser configuration significantly affect thermal uniformity and comfort level. Several recent studies have shown that HVAC configurations that generate uniformly distributed airflow can considerably reduce temperature fluctuations in learning spaces [3], while other experimental studies have emphasized the role of supply air velocity and temperature in transitional cooling processes and the formation of weak circulation zones [4]. For hot and humid climatic regions, zonal air supply systems have been demonstrated to significantly improve thermal comfort indices compared with conventional mixing ventilation [5].

However, most of these studies were conducted under climatic conditions and architectural contexts different from those of universities in Vietnam. In addition, recent studies have expanded thermal comfort analysis to perceptual and behavioral aspects, showing that traditional predictive models may underestimate the actual level of discomfort experienced by occupants [6]. Moreover, ventilation system design also affects acoustic conditions, thereby influencing concentration and learning quality [7]. Nguyen Minh Hoa [8], [9] investigated thermal comfort in educational and office spaces and energy optimization strategies for building air-conditioning systems, emphasizing the need to maintain acceptable indoor thermal comfort while reducing energy consumption. These studies indicate that thermal comfort assessment and energy-oriented HVAC operation are relevant research directions within the scope of the journal.

In practice, many classrooms in Southeast Asia still fail to achieve the recommended level of thermal comfort, even when equipped with HVAC systems, due to ineffective ventilation and prolonged hot and humid climatic conditions. Based on these research gaps, the present study focuses on analyzing the effects of supply air velocity and temperature on the thermal environment in typical university classrooms in Vietnam through CFD simulations using ANSYS software. The study evaluates temperature distribution, airflow patterns, and pressure fields under

different operating scenarios to identify optimal conditions that achieve a balance between thermal comfort and energy efficiency. The research results are expected to provide a scientific basis for the design and operation of HVAC systems in classroom environments in Vietnam and regions with similar climates. Within the scope of this study, thermal comfort assessment is conducted through physical environmental parameters, including air temperature and airflow velocity, obtained from CFD simulations and experiments. Human physiological and behavioral factors, such as metabolic rate or thermal adaptation, are not directly modeled but are considered indirectly through typical classroom operating conditions. Therefore, the research results reflect the characteristics of temperature and airflow distribution in the space and provide a basis for indirectly assessing thermal comfort conditions, rather than a comprehensive evaluation of human responses.

2. Methodology

2.1. Numerical method

This study employed CFD to analyze the airflow field and thermal field in classroom A207 at Foreign Trade University, Ho Chi Minh City. The classroom was modeled with dimensions of 7200 × 9200 × 3800 mm (length × width × height) and a capacity of approximately 25–30 students. A Cartesian coordinate system was established with the origin located at one corner of the classroom floor, the x-axis along the length, the y-axis along the width, and the z-axis along the height. The geometric layout, including desks, chairs, the lectern, LED lights, display screens, and ventilation openings, was constructed based on actual measurements.

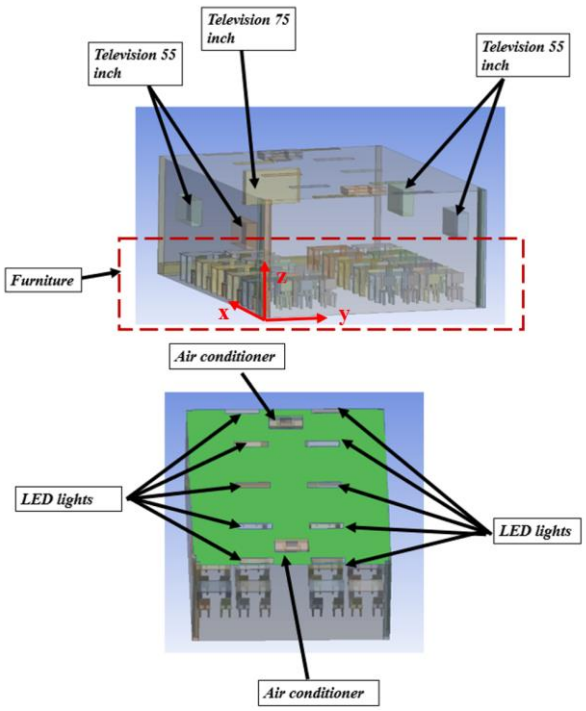

Figure 1. *Reconstructed CFD geometric model in ANSYS Fluent*

Two cassette air-conditioners were installed on the ceiling at an elevation of z = 3800 mm and arranged nearly symmetrically along the longitudinal axis of the room, with their centers located at x = 2400 mm, y = 4600 mm and x = 4800 mm, y = 4600 mm, respectively. Each cassette air-conditioner was modeled with supply air outlets in four directions, where the supply air velocity was applied at the outlets as the inlet boundary condition. The cold airflow was supplied from the outlets, propagated along the ceiling under the influence of the Coanda effect, then developed downward into the occupied zone and mixed with the indoor air. After heat exchange, the air was returned through the intake located at the center of each cassette air-conditioner, forming a local recirculation cycle.

After the geometric model was completed, the governing equations of airflow and heat transfer were applied within the computational domain. Air was assumed to be an incompressible fluid with constant thermophysical properties within the investigated temperature range, including a density of 1.2 kg/m³, a specific heat capacity of 1006 J/kg·K, a thermal conductivity of 0.026 W/m·K, and a dynamic viscosity of 1.8×10^{-5} kg/m·s. The flow was governed by the conservation equations of mass, momentum, and energy. The continuity equation ensures mass conservation, while the Navier–Stokes equations describe momentum transfer through the interactions among inertia, pressure gradients, and viscous forces.

Continuity equation:

$$\nabla \cdot (\rho \mathrm{u}) = 0 \tag{1}$$

Momentum equation Navier–Stokes:

$$\rho\left(\frac{\partial \mathrm{u}}{\partial t} + (\mathrm{u} \cdot \nabla)\mathrm{u}\right) = -\nabla p + \mu \nabla^2 \mathrm{u} + \mathrm{F} \tag{2}$$

Energy equation:

$$\rho c_p \left(\frac{\partial T}{\partial t} + \mathrm{u} \cdot \nabla T\right) = k\nabla^2 T + Q \tag{3}$$

The CFD simulations were performed using a pressure-based solver under steady-state flow conditions. Since the airflow in the classroom was affected simultaneously by forced convection from the supply air outlets and natural convection caused by temperature differences, the standard k–ε turbulence model was used to simulate the flow characteristics. This model solves two transport equations for the turbulent kinetic energy k and the turbulent dissipation rate ε:

$$\frac{\partial(\rho k)}{\partial t} + \frac{\partial(\rho k u_i)}{\partial x_i} = \frac{\partial}{\partial x_i}\left[(\mu + \frac{u_t}{\sigma_k})\frac{\partial \mathrm{k}}{\partial x_i}\right] + G_k - \rho\varepsilon \tag{4}$$

$$\frac{\partial(\rho \varepsilon)}{\partial t} + \frac{\partial(\rho \varepsilon u_i)}{\partial x_i} = \frac{\partial}{\partial x_i}\left[(\mu + \frac{u_t}{\sigma_\varepsilon})\frac{\partial \varepsilon}{\partial x_i}\right] + C_{1\varepsilon}\frac{\varepsilon}{k}G_k - C_{2\varepsilon}\rho\frac{\varepsilon^2}{k} \tag{5}$$

where G_k is the turbulent kinetic energy production term and μ_t is the turbulent viscosity. The k–ε model was selected because of its good numerical stability and suitability for indoor airflow problems. The effect of gravity was considered in the vertical direction z-axis, −9.81 m/s².

The inlet boundary conditions were set with supply air velocities of 1.22, 1.56, and 1.92 m/s, respectively, selected to represent the low, medium, and high operating modes of the cassette air-conditioner in practice. Since the velocity at the supply air outlet was not directly provided in the technical documentation, these values were inferred from the airflow rate and outlet area, with a typical velocity range of approximately 1–2 m/s. The corresponding supply air temperatures were 16°C and

18°C, depending on the operating case, while the louver angle of the cassette air-conditioner was fixed at 60°. This angle was defined as the angle between the airflow direction and the ceiling plane, allowing the airflow both to adhere to the ceiling due to the Coanda effect and to develop downward into the occupied zone.

The outlet boundary of the room was defined using a standard pressure condition of 101325 Pa. All wall surfaces were modeled with the no-slip condition applied to solid surfaces, where the airflow velocity at the wall was zero. Internal heat sources in the room, including LED lights and television screens, were incorporated into the model through corresponding heat flux densities based on the actual operating characteristics of the devices. Specifically, the LED lights and television screens were assumed to be made of aluminum, with heat flux densities of 90 W/m² over the surface area, similarly 120 W/m² for the 55-inch television surface and 150 W/m² for the 75-inch television surface.

The wall surfaces were assumed to be thermally inert because, under actual operating conditions, heat exchange through the walls is small compared with the effects of supply airflow and internal heat sources in the room. The SIMPLEC algorithm was used for pressure–velocity coupling to ensure stable convergence in low-velocity flow regions and recirculation zones. High-order spatial discretization schemes were applied to the momentum, turbulence, and energy equations to reduce numerical errors and improve the resolution of velocity and temperature gradients.

The convergence criteria were set to residuals of 10^{-6} for the energy equation and 10^{-5} for the continuity and momentum equations. Through this comprehensive methodology, the CFD simulation provides a reliable representation of airflow behavior and the thermal field in the classroom, serving as a basis for evaluating HVAC system performance under different operating scenarios.

2.2. Experimental setup for validation

To validate the reliability of the CFD simulation, an experimental measurement plan was conducted in the classroom using an ES35-SW temperature–humidity sensor, which employs an SHT35 chip with an accuracy of ±0.2°C for temperature and ±1.5% for humidity [10]. Before measurement, the electronic devices and air-conditioning system were operated for one hour to reproduce the typical thermal load of the classroom.

During the measurement sessions, the classroom was kept unoccupied and only one cassette air-conditioner was operated to eliminate heat effects from occupants, thereby isolating the impact of the HVAC system on the thermal field. Each experimental condition was maintained for 30 minutes to ensure a near-steady state, with the outdoor temperature approximately 34°C.

Table 1 presents a comparison of the average indoor temperature between the simulation and experimental results. The relative error ranged from approximately 0.34% to below 19%. The cases with a supply air temperature of 18°C showed small errors below 7%, whereas the cases with a supply air temperature of 16°C had higher errors. This discrepancy can be explained by the simplified assumptions applied in the CFD model, such as a sealed room, the exclusion of heat generated by the experimenter, the neglect of humidity, the assumption of thermally inert adiabatic walls, errors from the turbulence model, and the inherent nature of the simulation method.

Nevertheless, the model still reproduced the correct trend of the effects of operating parameters on the indoor thermal field. Therefore, the CFD model was considered to have suitable reliability for the objectives of qualitative investigation and relative comparison, and it can be used to analyze the effects of HVAC operating parameters on temperature distribution and comfort conditions in subsequent scenarios.

Table 1. *Comparison between experimental and simulation results*

Temperature (°C)	Opening angle (°)	Velocity (m/s)	Simulation (°C)	Experiment (°C)	Error (%)
16	60	1.22	23.00	28.25	18.5
16	60	1.56	21.30	26.24	18.8
16	60	1.92	20.60	25.28	18.5
18	60	1.22	25.00	25.09	0.34
18	60	1.56	23.50	25.22	6.80

2.3. Grid independence test and convergence

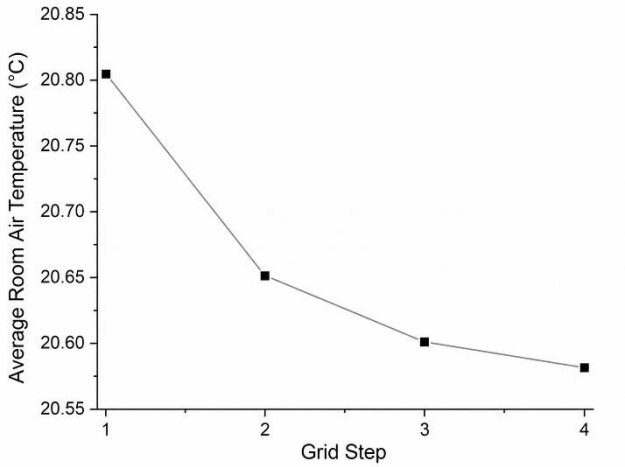

Figure 2. *Comparison of average classroom air temperature as a function of mesh steps*

Before conducting the full CFD simulations, a grid independence study was performed to ensure that the numerical results were not dependent on the computational mesh density. The average indoor temperature was selected as the indicator for evaluating grid sensitivity under a representative operating condition with a supply air velocity of 1.22 m/s, a supply air temperature of 16°C, and an opening angle of 60°.

Four corresponding mesh levels were used to compare accuracy and computational cost, in which mesh level 1 consisted of 723,733 elements and was gradually refined. The error convergence process showed a stable reduction in the investigated variable. The average indoor temperatures corresponding to three mesh levels, namely 3,752,218 elements mesh level 2, 13,565,029 elements mesh level 3, and 21,702,602 elements mesh level 4, are presented in Figure 2.

The comparison shows that further mesh refinement beyond mesh level 2 did not significantly change the predicted results; specifically, the temperature difference between mesh level 2 and mesh level 4 was only 0.009%. Therefore, mesh level 2 was selected for the subsequent simulations to ensure a reasonable balance between accuracy and computational efficiency.

After establishing a computational mesh that satisfied the grid independence criterion, the physical boundary conditions were set in accordance with the experimental environment, in which the outdoor temperature was recorded at 34°C. The combination of the validated mesh and the convergence criteria of the problem provides a consistent and reliable CFD simulation framework for the subsequent analyses.

3. Results and discussion

3.1. Effect of supply air temperature on thermal comfort

The temperature fields at a height of 60 cm in Figure 3 clearly show the effects of supply air velocity and temperature on temperature distribution in the occupied zone. At a supply air temperature of 16°C (Figure 3a–c), when the velocity increased from 1.22 m/s to 1.56 m/s and 1.92 m/s, the average temperature decreased considerably and the temperature distribution became more uniform. The increase in airflow momentum allowed the cold air jet to penetrate deeper into the space and enhanced mixing, thereby reducing thermal stratification. However, the improvement between 1.56 m/s and 1.92 m/s was not significant, indicating that the cooling effect tended to become saturated as the velocity continued to increase.

When the supply air temperature increased from 16°C to 18°C (Figure 3d–e), the indoor temperature increased markedly and higher-temperature regions appeared, because the reduced temperature difference weakened the buoyancy force and the downward penetration capability of the cold air jet. In general, supply air velocity plays a dominant role in airflow distribution and mixing intensity, while supply air temperature determines the overall temperature level in the room. The case with a medium velocity of 1.56 m/s combined with a low supply air temperature showed a good balance between cooling performance and thermal uniformity.

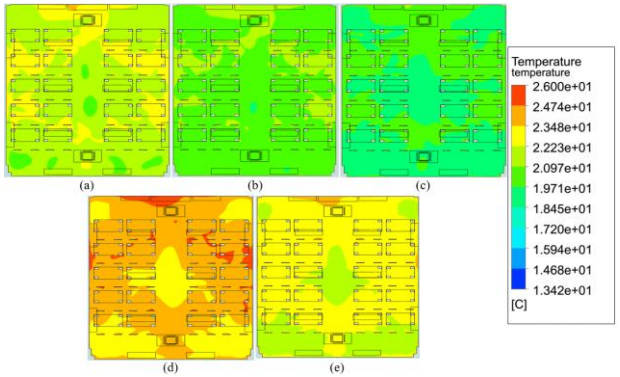

Figure 3. *Temperature distribution at a height of 60 cm with a discharge angle of 60° under different airflow velocity and supply temperature conditions: (a) 1.22 m/s, 16°C; (b) 1.56 m/s, 16°C; (c) 1.92 m/s, 16°C; (d) 1.22 m/s, 18°C; (e) 1.56 m/s, 18°C*

The results from Figure 3 show that supply air velocity and temperature directly affect temperature distribution in the classroom. A higher velocity increases the momentum of the air jet, improves penetration capability and mixing intensity, thereby reducing thermal stratification and increasing thermal uniformity. Meanwhile, a higher supply air temperature reduces cooling performance due to the smaller temperature difference.

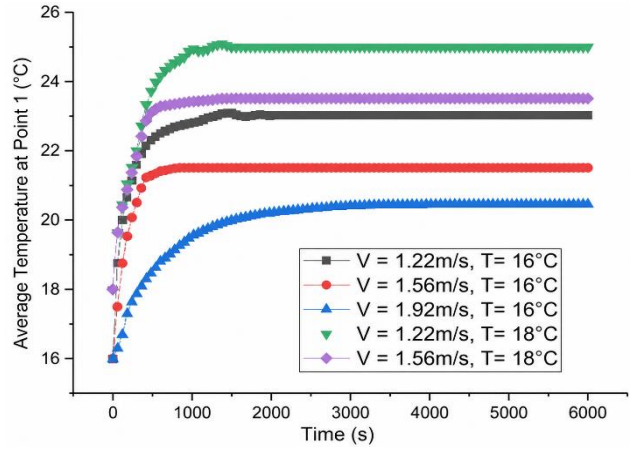

(a)

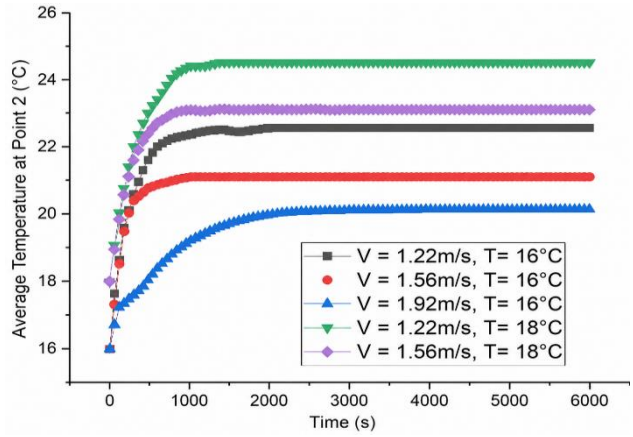

(b)

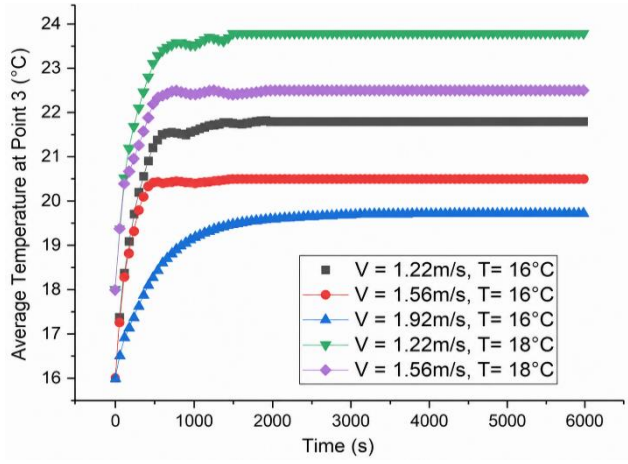

(c)

Figure 4. *Time histories of average temperature at the monitored points: (a) Point 1; (b) Point 2; (c) Point 3*

To evaluate unfavorable conditions in detail, three monitoring points were selected at representative

locations near regions where thermal stagnation is likely to occur, with their specific coordinates presented in Table 2. This arrangement allows the temperature trend in poorly ventilated regions to be reflected while still ensuring representativeness for the entire space. The temporal temperature variations at these points (Figure 4) show the transitional cooling process and the achievement of a near-steady state after approximately 1000–1500 s.

At a supply air temperature of 16°C, when the velocity increased from 1.22 m/s to 1.56 m/s and 1.92 m/s, the temperatures at the monitoring points decreased by approximately 2–2.5°C, reflecting the role of airflow momentum in improving temperature distribution. However, the difference between 1.56 m/s and 1.92 m/s was not significant, while the velocity of 1.56 m/s already ensured that the temperature remained within the comfort range and was stable over time. Overall, the medium velocity combined with the low supply air temperature showed a reasonable balance between cooling performance and comfort conditions, whereas increasing the velocity to a higher level provided only limited improvement.

Table 2. *Temperature-monitoring point's locations*

Location	x(mm)	y(mm)	z(mm)
1	176	0	0
2	423	850	66
3	146	0	72

The results indicate that supply air temperature and velocity simultaneously affect temperature distribution and comfort level in the classroom. A low supply air temperature increases the temperature difference and improves cooling performance, while a higher supply air velocity increases airflow momentum, contributing to reduced thermal stratification and enhanced air mixing. However, when the velocity exceeds a certain value, the improvement in temperature becomes insignificant. Therefore, the results show that the combination of a low supply air temperature and a medium velocity provides optimal performance, ensuring a balance among cooling capacity, thermal uniformity, and comfort conditions in the learning space.

3.2. Effect of supply air velocity on thermal comfort

The airflow characteristics in classroom A207 with a 60° discharge angle are shown in Figure 5 and Figure 6 through the temperature fields, velocity fields, and iso-surfaces, allowing the airflow distribution regions and the propagation extent of the cold air jet within the space to be clearly identified. Under the low-velocity condition of 1.22 m/s (Figure 5a and 6a), the air jet tended to adhere to the ceiling due to the Coanda effect and propagated horizontally before losing momentum and descending into the lower zone. The iso-surfaces show that the influence region of the airflow was still limited, leading to the presence of low-velocity regions and the possible formation of thermal stagnation zones.

When the velocity increased to 1.56 m/s and 1.92 m/s (Figure 5b–c and 6b–c), the propagation range of the air jet expanded considerably. The iso-surfaces indicate that the effective velocity region covered deeper into the occupied zone, while enhancing air mixing and reducing low-velocity regions. However, the difference between these two cases was not large, indicating that the improvement effect tended to decrease gradually as the velocity continued to increase.

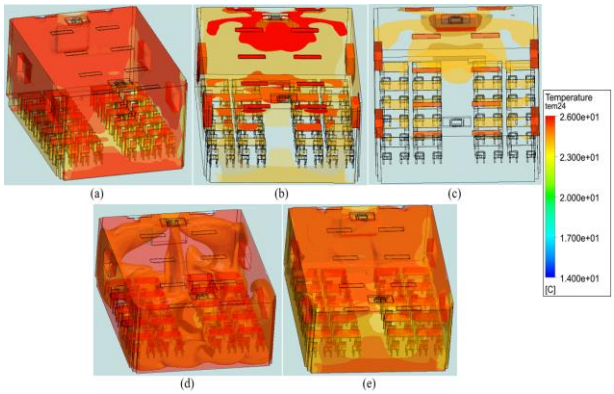

Figure 5. *Temperature distribution in the room at a discharge angle of 60° under different airflow velocity and supply temperature conditions: (a) 1.22 m/s, 16°C; (b) 1.56 m/s, 16°C; (c) 1.92 m/s, 16°C; (d) 1.22 m/s, 18°C; (e) 1.56 m/s, 18°C*

Meanwhile, when the supply air temperature increased from 16°C to 18°C (Figure 5d–e and 6d–e), the airflow structure and velocity distribution remained almost unchanged, as reflected by the similar shapes of the iso-surfaces. This indicates that the spatial development of the airflow mainly depends on mechanical momentum, while the effect of supply air temperature on the velocity field is secondary and occurs through buoyancy.

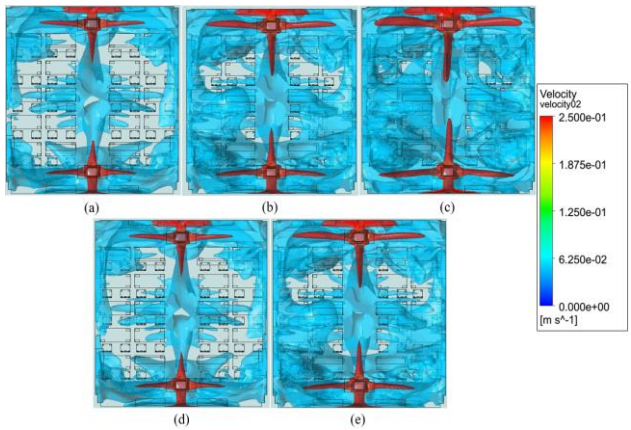

Figure 6. *Air velocity distribution in the room at a discharge angle of 60° under different airflow velocity and supply temperature conditions: (a) 1.22 m/s, 16°C; (b) 1.56 m/s, 16°C; (c) 1.92 m/s, 16°C; (d) 1.22 m/s, 18°C; (e) 1.56 m/s, 18°C*

In general, the results show that supply air velocity is the main factor governing the penetration capability and airflow distribution in the room. The medium-velocity case of 1.56 m/s showed a reasonable velocity distribution region, ensuring coverage of the occupied zone while maintaining the velocity values within the comfort limits. Thus, this case achieved a balance among ventilation effectiveness, temperature distribution, and comfort conditions.

4. Conclusion

This study employed CFD to evaluate the effects of supply air velocity and temperature on airflow organization, temperature distribution, and comfort conditions in a classroom using cassette air-conditioners. The CFD model reproduced the overall trend of the experimental results, with relative errors ranging from 0.34% to 18.8%, making it suitable for qualitative analysis and relative comparison.

The results show that supply air velocity plays a dominant role in airflow characteristics and air mixing intensity. Increasing the velocity from 1.22 m/s to 1.56 m/s clearly improved temperature distribution and reduced stagnant zones, whereas further increasing the velocity to 1.92 m/s provided only limited improvement. Meanwhile, reducing the supply air temperature from 18°C to 16°C enhanced cooling performance but mainly affected the overall temperature level, with little influence on the airflow structure.

Considering all factors, the medium-velocity case of 1.56 m/s combined with a supply air temperature of 16°C showed a reasonable balance among cooling capacity, thermal uniformity, and comfort conditions in the occupied zone. Although a lower supply air temperature may reduce the coefficient of performance COP of the air-conditioning system, the results indicate that improving airflow distribution through velocity optimization can reduce the need to excessively lower the supply air temperature.

It should be noted that the low supply air temperature cases in this study were intended only to investigate trends in their effects on airflow organization and temperature distribution, rather than to recommend long-term operating conditions for HVAC systems. Therefore, instead of relying solely on low temperature to achieve cooling performance, optimizing airflow organization allows comfort conditions to be maintained with more reasonable energy consumption.

These results demonstrate the practical significance of the study in supporting the design and operation of HVAC systems. Simultaneous optimization of supply air velocity and discharge direction can improve energy efficiency, limit COP reduction caused by deep cooling, and ensure comfort conditions in learning spaces under hot and humid climates.

Acknowledgements: This work was supported by Foreign Trade University under Research Project No. NTCS2024-15.

REFERENCES

[1] ANSI/ASHRAE Standard 55, *Thermal Environmental Conditions for Human Occupancy*, American Society of Heating, Refrigerating and Air-Conditioning Engineers, Atlanta, GA, USA, 1992.

[2] International Organization for Standardization, *Ergonomics of the Thermal Environment—Analytical Determination and Interpretation of Thermal Comfort Using Calculation of the PMV and PPD Indices and Local Thermal Comfort Criteria*, ISO 7730, Geneva, Switzerland, 2005.

[3] A. M. Hanafi, T. A. Abdo, N. A. Abbass, Y. M. Diab, M. G. Abdelfatah, and M. A. Ibrahim, "Optimizing thermal comfort and air quality in university classrooms: A CFD-based comparative analysis of HVAC configurations," *Journal of Engineering Research*, vol. 2, no. 1, pp. 17–31, Jan. 2025.

[4] W. Zhao, S. Lestinen, P. Mustakallio, S. Kilpeläinen, J. Jokisalo, and R. Kosonen, "Experimental study on thermal environment in a simulated classroom with different air distribution methods," *Energy and Buildings*, vol. 43, Art. no. 103025, Nov. 2021.

[5] "The influence of zonal air supply on thermal comfort in a classroom located in a hot and humid environment: A case study from Jeddah, Saudi Arabia," *Scientific Reports*, vol. 5, Art. no. 526, 2024.

[6] T. D. Mustapha, A. S. Hassan, M. H. A. Nasir, F. Khozaei, and Y. Arab, "From perception to prediction: A comparative study of thermal comfort assessment techniques in school facilities," *Building and Environment*, vol. 313, Art. no. 114233, Jun. 15, 2024.

[7] Q. Y. Nguyen, T. T. Le, and H. M. A. Pham, "*Thermal comfort sensation in naturally ventilated lecture rooms*," research report, Ho Chi Minh City University of Technology, Ho Chi Minh City, Vietnam.

[8] N. M. Hoa, "*Evaluation of Temperature Comforts at Tra Vinh University". The University of Danang - Journal of Science and Technology*, vol. 18, no. 9, pp. 17–21, Sep. 2020.

[9] N. M. Hoa, "*Optimization of Energy Used by Air-Conditioning Systems in Buildings Using Model Predictive Control Strategy". The University of Danang - Journal of Science and Technology*, vol. 19, no. 5.1, pp. 39–43, May 2021. https://jst-ud.vn/jst-ud/article/view/7497.

[10] EPCB Vietnam, "Why choose the RS485 Modbus RTU ES35-SW temperature and humidity sensor," *EPCB Vietnam*, May 2023. [Online]. Available: https://epcb.vn/blogs/news/tai-sao-chon-cam-bien-nhiet-do-do-am-rs485-modbus-rtu-es35-sw [Accessed: Jun. 3, 2023]